LAWRENCE
LIVERMORE
NATIONAL
LABORATORY

LLNL-PROC-462148

Temperature activated absorption during laser-induced damage: The evolution of laser-supported solid-state absorption fronts

C. W. Carr, J. D. Bude, N. Shen, P. Demange

November 15, 2010

SPIE Laser Damage Conference
Boulder, CO, United States
September 26, 2010 through September 29, 2010

Disclaimer

This work performed under the auspices of the U.S. Department of Energy by Lawrence Livermore National Laboratory under Contract DE-AC52-07NA27344.

Temperature activated absorption during laser-induced damage: The evolution of laser-supported solid-state absorption fronts

C.W. Carr, J.D. Bude, N. Shen, P. Demange

Lawrence Livermore National Security, LLC,

Lawrence Livermore National Laboratory, Livermore, CA

Abstract

Previously we have shown that the size of laser induced damage sites in both KDP and SiO_2 is largely governed by the duration of the laser pulse which creates them. Here we present a model based on experiment and simulation that accounts for this behavior. Specifically, we show that solid-state laser-supported absorption fronts are generated during a damage event and that these fronts propagate at constant velocities for laser intensities up to 4 GW/cm^2. It is the constant absorption front velocity that leads to the dependence of laser damage site size on pulse duration.

We show that these absorption fronts are driven principally by the temperature-activated deep sub band-gap optical absorptivity, free electron transport, and thermal diffusion in defect-free silica for temperatures up to 15,000K and pressures < 15GPa. In addition to the practical application of selecting an optimal laser for pre-initiation of large aperture optics, this work serves as a platform for understanding general laser-matter interactions in dielectrics under a variety of conditions.

Keywords: Absorption mechanisms, Surface damage, initiation fused silica.

* Correspondence: Email: carr19@llnl.gov Mailstop: L-592, Telephone: 925-422-8755, Fax: 925-422-5099

I. INTRODUCTION

In recent years, a good deal of work has been presented at this conference characterizing optical damage as a function of the laser parameters used to initiate it. It has been shown that for damage initiated as a result of extrinsic precursors, parameters such as laser spot size, pulse shape, photon energy (E_ν), and sample temperature can have a significant impact on the behavior of damage initiation and growth. The physical mechanisms by which theses parameters affect damage initiation and growth is still not well understood[1-5]. Isolating the mechanisms behind laser-induced damage is difficult

because damage is a complex event governed by a succession of physical processes starting with energy deposition (initiation) at a precursor which results in high temperatures and pressures, concluding with material ejection and fracture[1-6]. In this work we propose that the size of exit surface damage in silica corresponds to an increase in absorbing volume and is the result of a laser–supported solid-state absorption front caused by temperature activated absorption.

Our model for energy deposition via an expanding laser-driven absorption front initially came from the observation that damage site size increases linearly with pulse duration for both bulk damage in KDP and exit surface damage in SiO_2 (see figure 1), and recent work that showed the absorbing mechanism changes during the pulse which results in an expansion of the absorbing volume[1,7,8]. Because damage size increases linearly with the pulse duration, it is likely that new absorbing material is generated during the pulse. Temperatures during a laser damage event have been measured to be as high as 10,000K[9], and SEM images of damage sites show evidence that material is ejected through explosive boiling (e.g., see Fig. 2 below). Clearly, laser energy has been deposited by absorption in these high temperature regions; we argue below that energy is deposited in these regions because they are at high temperature. As the absorbing volume expands, we refer to this growing absorbing region as an absorption front (AF).

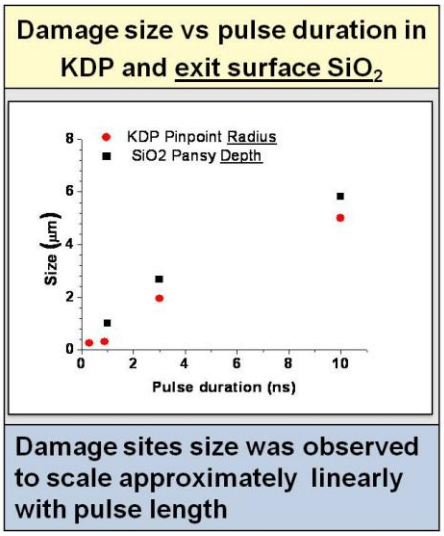

Figure 1. Both bulk damage (pinpoint) in KDP and exit surface (Pansy) damage on SiO_2 optics have been previously observed to increase in size when exposed to longer pulse durations.

A number of hypotheses were proposed which were subsequently shown to be unlikely. Absorption along a shock-front was disproven because the velocity of the site expansion was significantly slower than the speed of sound. Further evidence against absorption along a shock front came from experiments which measured the damage site size for surfaces subjected to double pulses. In 2007 we showed that two flat in time pulses separated by a few ns did not produce sites of enhanced size. If energy had been deposited on a shock front, a slight pause in laser illumination would have allowed the shock front to expand outward before the second pulse arrived, producing larger sites. As no size enhancement was observed for delays ranging from 250 ps to 16 ns, these measurements indicated that energy deposition cannot occur on a shock front launched during absorption. Absorption on

propagating fractures and by diffusing electrons were also shown to be unlikely because they indicated a sub-linear pulse length dependence of the site size.

In 2007, a different mechanism was proposed to explain the growth of an absorption front. It was found that simulation models of heat transport during damage which included temperature-activated absorption and phonon thermal diffusion predicted generation of an absorption front, and that it would move with constant velocity. However, these models predicted that the absorption front velocity was slower than that estimated by the experiments above. The simulations also predicted that the absorption front velocity depended more strongly on the intensity of the laser than these early measurements indicated[3,7].

In this work we will show that for surface damage in silica, a temperature activated absorption front is driven by a combination of phonon thermal conductivity with a significant contribution due to thermal transport by free elections. We will show that the addition of a free electron component to thermal conductivity reconciles measured and simulated absorption front velocities as well as peak temperatures. Enhancements to our measurement techniques have improved our measurements of absorption front velocities which now are much closer than those predicated by simulation.

In order to accurately determine the extent of the absorption front from surface damage sites, we identify the extent of the damage sites which experienced high temperatures. Figure 2 shows that high temperatures are constrained to the central core of the damage sites. The extent of a temperature activated growth front is determined by the high temperature region. Therefore, the extent of the growth front is indicated by the molten core of the damage sites. Past measurements have used the region of fracture surrounding the core as a metric of site size. Here we will exclusively use SEM measurements of the core region which more accurately reflect to true extent of the absorption front.

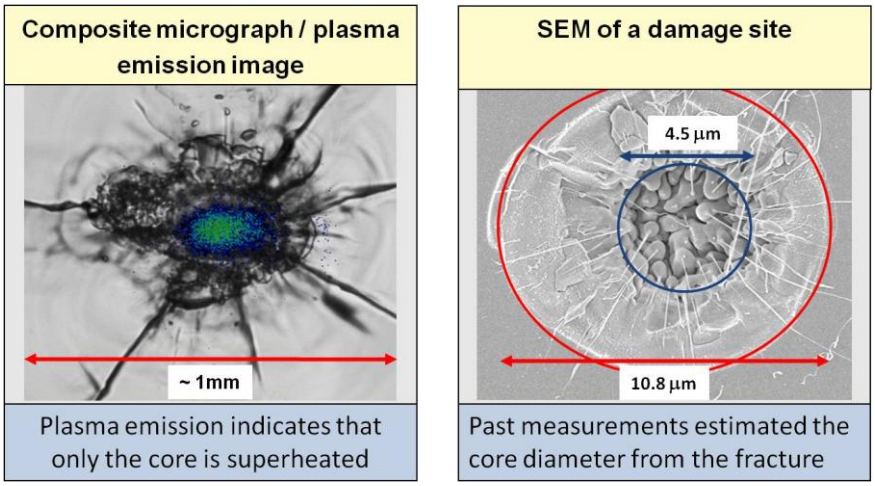

Figure 2. The figure on the left shows that the high temperature region is confined to the central core of the damage site. The figure on the right illustrates the difference in measured site size depending on if the fracture surrounding the molten core is included. In this work, only the core will be used to determine site size

II. Experiment

Damage was initiated on two-inch diameter, fused silica windows polished by CVI-Melles Groit. All samples were cleaned with detergent and an ultra-sonic DI water rinse. The Optical Science Laser facility used single laser pulses with various temporal pulse shapes to expose regions of the samples[6]. The laser was slowly focused (f20) and had a higher fluence on the exit surface of the sample where all the damage examined here was initiated. No damage was observed on the input surface of any of the samples. The 1-cm diameter laser spot produced by OSL in the configuration used is very large compared to the size of the damage sites which range in size from a few to a few tens of microns (see below). Because damage is initiated on the exit surface, vaporized and ejected material does not interfere with the interaction of the laser with the bulk silica.

The pulse shapes used in the experiment were composed of two consecutive pulses of constant intensity. These two component pulses were used to separate the evolution of the absorption front from the initial energy deposition at the precursor. The first part of the pulse is a short, 2-ns, 8-GW/cm^2 pulse designed to initiate damage and to create a consistent (in size) heated volume from which to propagate an absorption front. We refer to this 2 ns pulse as the Absorption Front Initiator pulse (AFI pulse). The AFI pulse and an SEM of a typical damage site created by it can be seen in figure 3. Damage sites created by the AFI pulse have a mean core diameter of 2.1 μm with a standard deviation of 0.3 μm.

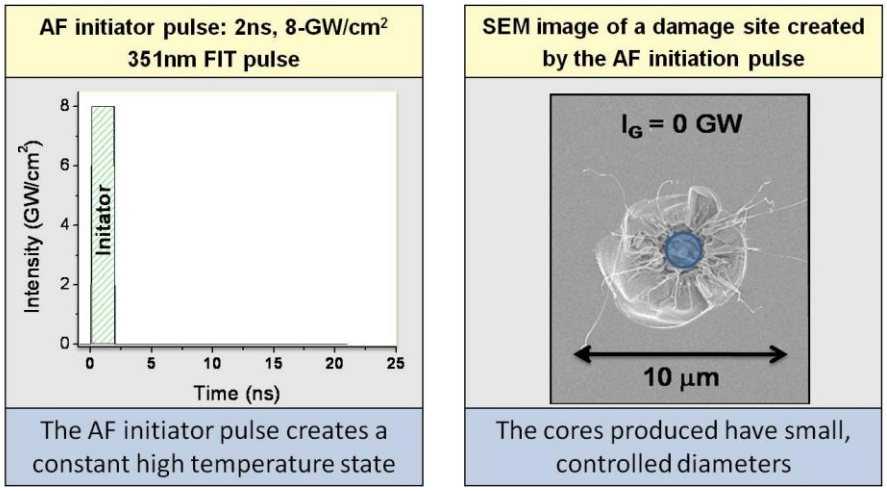

Figure 3. The circle in the SEM on the right is the average size of 40 damage sites created by the AFI pulse. The particular site shown in the figure was chosen because it had a median diameter core.

The second part of the pulse is a low intensity growth foot which immediately follows the AFI. The growth part of the pulse is used to probe the expansion of the absorption front under controlled conditions. Figure 4 shows a schematic representation of the complete pulse as well as five examples of sites created with different lengths and intensities of growth feet. The central circle in each image is the average size of the sites created by the AFI pulse alone. The lager circle is the average size of 10 to 40 sites examined by SEM. In each case the site with the core diameter most closely equal to the diameter was chosen.

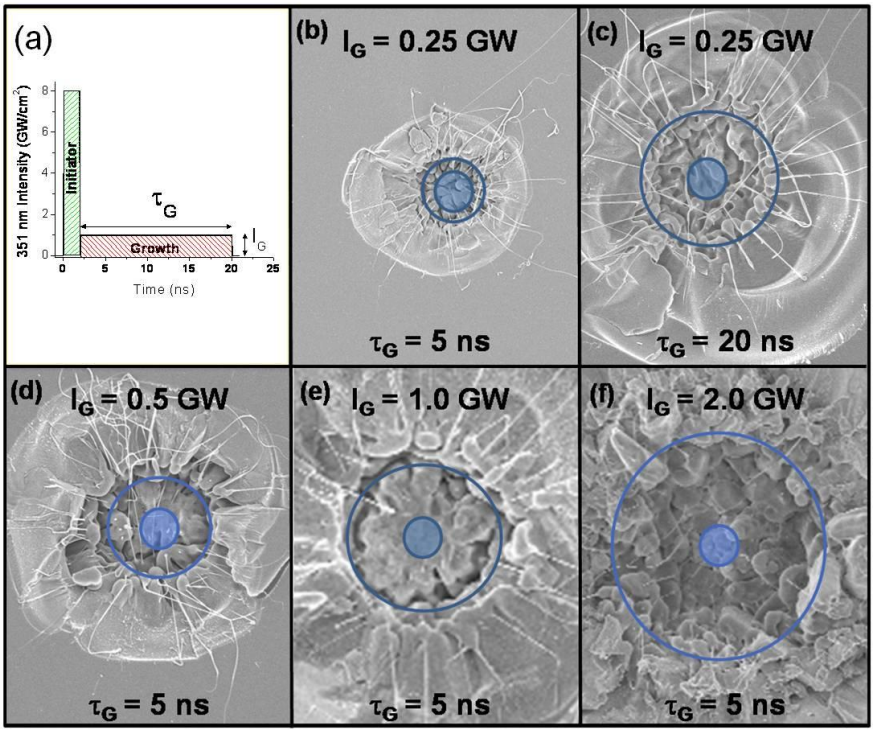

Figure 4. a. A schematic of the pulse shape used to initiate the damage sites seen if b-f. The 8-GW initiator part is fixed, while the duration (τ_G) and intensity (I_G) of the growth foot are varied from experiment to experiment.

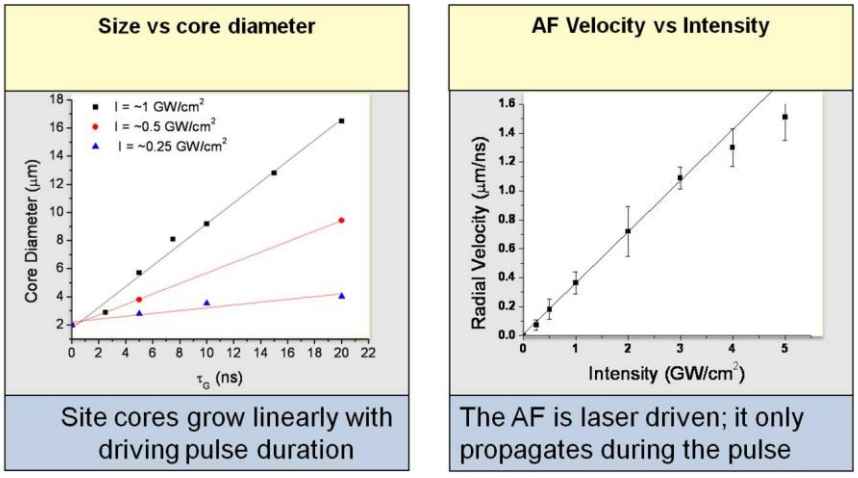

Figure 5. The figure on the left shows that for a fixed intensity site size increases linearly with pulse duration, and that the rate at which they increase is dependent on intensity. The figure on the right shows that the rate of size increase (velocity) has a slightly sub-linear dependence on intensity

The average core diameters for three different intensities of foot can be seen as a function of foot duration in the left hand side of figure 5. The Y-intersect of ~ 2 microns is indicative of the starting core size (from the AFI pulse). The linear increase in diameter with pulse duration indicates that for a fixed intensity, the absorption front propagates at a constant velocity. The right side of figure 5 shows the absorption front velocity as a function of intensity.

III. THE TEMPERATURE-ACTIVATED ABSORPTION MODEL

Our premise is that that constant velocity absorption front indicated in figure 5 is driven by temperature-activated bulk absorption. This is supported by two independent observations. Laser-induced surface damage has been generated in pristine silica for fluence significantly below the intrinsic damage threshold when the surface is heated to a temperature of ~2,200K[7]. This indicates that the absorptivity of defect-free intrinsic silica, $\alpha_{INT}(T)$, is strongly enhanced with temperatures as low as 2,200K, allowing thermal run-away under pulsed laser illumination.

The effect of temperature activated absorption during a damage event is illustrated by equation (1) which includes energy deposition, heat flow and simple photon transport, but not full radiation transport. Initially, we solved (1) in one spatial dimension (1D) to explore the effects of temperature-activated absorption on the evolution of energy absorption. Here, $\kappa_{PH}(T)$ is the silica phonon thermal conductivity, $C_p(T)$ is the heat capacity, and ρ is density (values for T up to ~2,000K[10]); t is time during the laser pulse, and x is position below the surface.

$$(C_p(T)\rho)\frac{\partial T}{\partial t} = \nabla \bullet (\kappa_{PH}(T)\nabla T) + G_{FE}(x) + I_L \alpha_{INT}(T) \qquad (1)$$

$$\frac{\partial I_L}{\partial x} = -\, I_L \alpha_{INT}(T)$$

We model initiation occurring at t=0 on a 200 nm precursor and therefore employ the initial boundary condition T(x,t=0)=8,000K for x<200nm. $C_p(T)$ is modeled elsewhere[11] for temperatures above 8,000K. I_L is the laser intensity and is constant in time. The temperature activated absorption is modeled on the exit surface, e.g. the laser propagates through the bulk before illuminating the surface. The free electron contribution to thermal diffusion (G_{FE}) is defined in detail in reference [8]. Cooling by radiation and evaporation were found to have little effect on energy deposition on the ns time scale. We note that the initial size of the precursor is not critical to modeling the evolution of the absorbing volume and would only represent an offset in time. The assumption of a 200 nm precursors is biased both on past work[5] and on minimum size of damage sites observed with very short (140 ps) pulses[12].

As the temperature of a dielectric increases, phonon vibrations generate transient structural disorder and form localized electronic states in the gap, sometimes described as an exponentially decaying Urbach tail. The tail states are separated from continuum free-electron states by the "optical gap" E_O which is reduced by increasing temperature. This process is known as band-gap, E_G, narrowing. For absorption of a photon of energy E_ν, this behavior has been modeled[11] as:

$$\begin{aligned} \alpha_{INT}(E_\nu) &\propto \exp(E_\upsilon / E_u) && E_\upsilon < E_o \qquad (2) \\ &\propto (E_\upsilon - E_o)^2 / E_\upsilon && E_\upsilon \geq E_o \end{aligned}$$

where $E_O(T)=E_G-AT$, $E_U(T) = B + CT$, E_G~9eV is the low temperature band gap, and A,B and C are constants. We fit C so that α_{INT}(2,200K) is large enough to support thermal runaway under the conditions of [7], and find $C=1.8\times10^{-4}$eV/K, close to $C=1.4\times10^{-4}$ reported elsewhere[13]. Figure 6 shows the resulting temperature dependence of absorptivity ($\alpha_{INT}(T)$) for photons with E_ν=3.55eV.

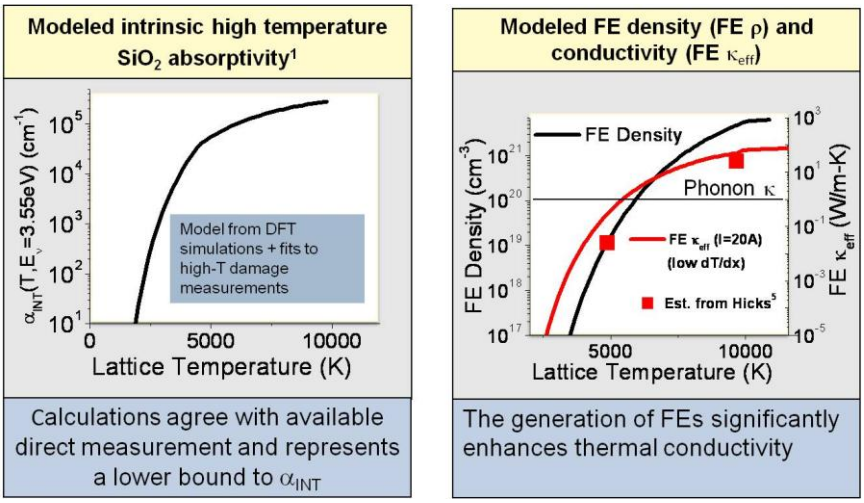

Figure 6. Left; temperature activated absorptivity modeled as described above. Right; temperature activated Free Electron (FE) density and the effective thermal conductivity due to free electrons.

An additional effect to the attenuation of E_0 at high temperatures is the population of free electron states. To be consistent with $\alpha_{INT}(T)$, the conduction and valence bands, E_C and E_V, follow the optical gap: $E_C-E_V=E_O$. We assume the Fermi level, $E_F=0$, is in the middle of the optical gap in order to ensure charge neutrality, so that $E_C(T)-E_F=E_0(T)/2$. The free electron density of states, the wave-vector (k) dependent velocity, v(k), and free electron energy relative to the band edge, E(k), are computed using a simple effective mass approximation fit to the silica band structure[14]. This model predicts that free electron densities increase dramatically between 5,000K and 10,000K as can be seen on the left in figure 6.

In this model, free electrons are confined to the hot region by a large increase in $E_C(T)$ from high to low temperature[15]. This restriction on mobility does not preclude the free electrons from effectively adding to the thermal transport. In a given region, the hottest electrons are able to move against the effective electric field. However, after undergoing a number of scattering events, the electrons lose thermal energy, causing them to be pushed back to the location from which they originated. So, although there is not a significant net flow of electrons, the scattered electrons do affect transport heat (see figure 7). In the limit where the temperature gradient becomes small, we can extract an effective thermal conductivity from G_{FE}; this effective thermal conductivity is shown in figure 6 on the right and compares reasonably well with estimates taken from the shock measurements of[5].

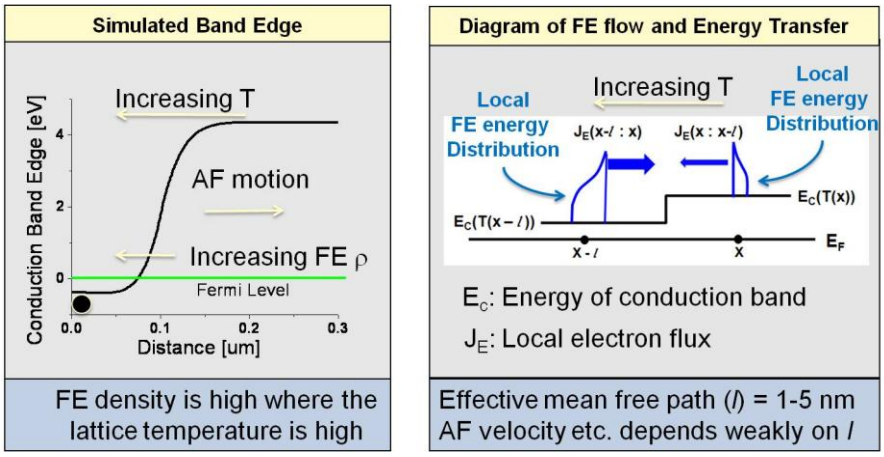

Figure 7. Left; A schematic of the band edge near an absorbing precursor (represented by the black dot) which has begun to heat the surrounding lattice. Right; a close up view of an arbitrary point along the simulated band edge where the continually changing band edge has been approximated by a discrete step to illustrate the local flow of heat and free electrons.

Simulations were performed for the geometry of a beam much larger than the absorber (using a finite element explicit method with error control) for two cases: with only phonon diffusion (G_{FE}=0) and with both phonon and FE thermal diffusion. Fig. 8 shows results for I_L=1GW/cm^2. The 8,000K surface layer (precursor) activates $\alpha_{INT}(T,x=0)$ leading to high energy deposition. As the surface layer get hotter, heat diffusion begins to activate $\alpha_{INT}(T,x=\delta)$ at points just next to the layer. $T(x=\delta)$ increases beyond 8,000K, and pushes energy deposition back further. This process continues while the laser is on creating a laser-supported solid-state AF.

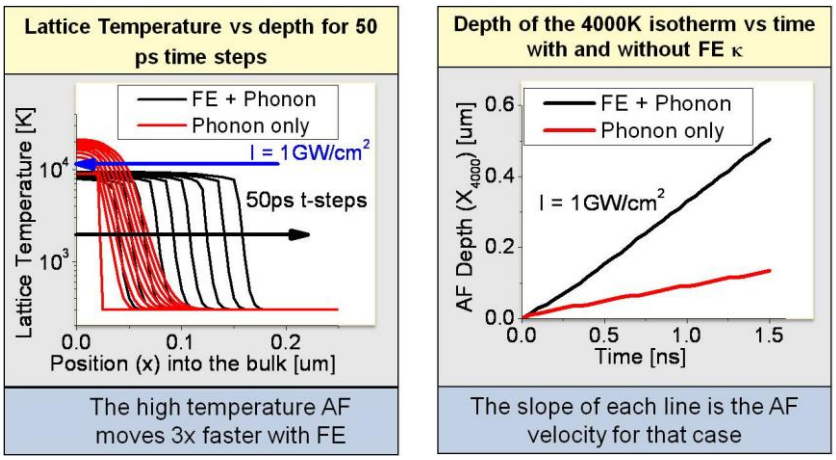

Figure 8. Left; Shows the calculated temperature profile in 50 ps time steps for the modle using Phonon thermal conductivity only and with the addition of the thermal conductivity by free electrons. Right; The location of the 400K isotherm is plotted as a function of time to better illustrate the velocity differences induced by including the free electron component of the thermal conductivity

The position of the AF, X_{4000}, defined as the depth where T > 4,000K (>>boiling point) for x≤ X_{4000}, moves linearly with time resulting in a constant AF velocity, $V_F = dX_{4000}/dt$ as shown in figure 8. Other isotherms above 4000K have indistinguishable behavior. Without FE contributions, both T_{max} and V_F increase, and T_{max} can then become much larger (>40,000K) than measured values[16]. When the pulse

(and energy deposition) ends, there is very little further thermal diffusion and $V_F \rightarrow 0$; hence, the absorption front is laser supported.

In order to relate the physics of 1D absorption fronts to measured damage sites, we included temperature-activated absorption and free electron thermal diffusivity in 2D axial symmetric (R=radial, x=axial or depth direction) hydrodynamic (HD) simulations which were solved using ALE3D[23]. ALE3D uses an equation of state model based on fits to the high pressure fused silica Hugoniot and the model described by Young and Corey[17]. While not comprehensive, these HD simulations show similar behavior to both the experimental observations and 1D calculations, which helps corroborate the overall physical picture proposed here. It is expected that a more refined picture of damage growth can be obtained by more systematic HD simulations which include the effects highlighted in this work.

The HD simulations here include photon transport, and $\alpha_{INT}(T)$ and k_{PH} as in equation (1) but approximate G_{FE} with a $k_{eff}(T)$ similar to that defined above. To mimic the 1D case, the initial condition was a 8,000K, 100nm hemisphere at the surface (x=0); I_L propagated in x through the bulk towards x=0. Simulations were performed up to 2ns for I_L =1,2GW/cm^2. As in the 1D case, we found that an absorption front formed while the laser was on, and that it propagated with linear V_F away from the initial heated region; furthermore, the absorption front expanded in all directions. Fig. 9 shows the simulated temperature profile after 2ns with I_L=2GW/cm^2. The size of the absorption front is defined by the maximum extent of the region > 4,000K in the R- and x-directions. Radial and axial absorption front velocities, V_{FR} and V_{FX} were 0.75μs/ns, and 1.05μm/ns respectively.

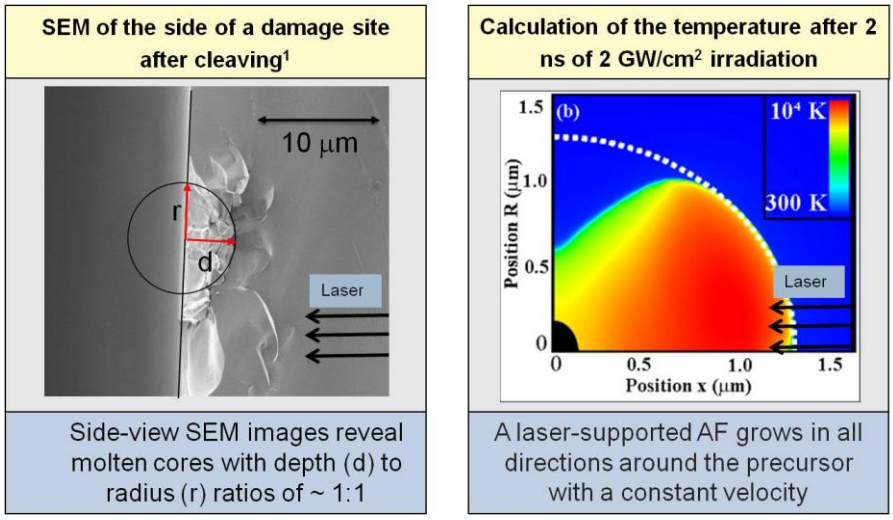

Figure 9. The results from theses preliminary HD simulations, the results from the 1D simulations, and the experimental measurements are compared in figure 10.

In figure 10 we compare the experimental measurements from figure 5 with the 1D calculation for both with and without a free electron component to the thermal conductivity. We see that the 1D model with the free electron component of thermal conductivity agrees very well with both the hydro calculation as well as the experimental measurements.

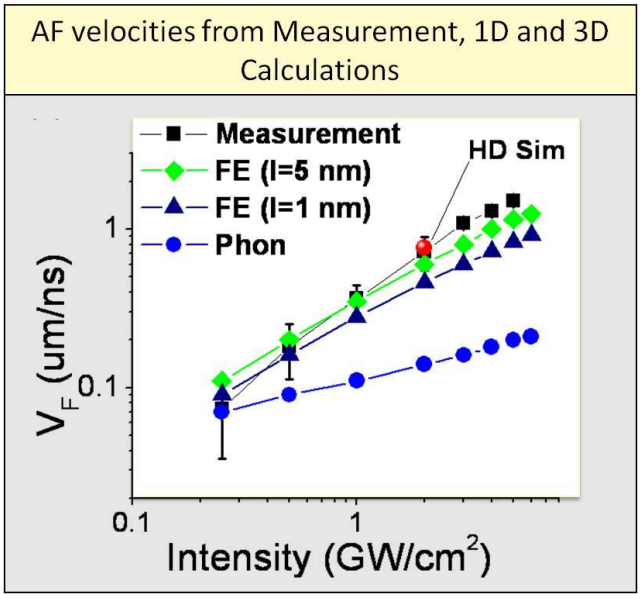

Figure 10. Comparison of absorption front velocity's from the 1D simulation with and without the free electron component of thermal conductivity, the measurement, and a single point from the 3d HD simulation

IV Summary

We have presented evidence here to show that an absorbing precursor reaches several thousand degrees, a laser-driven absorption front forms in the bulk SiO_2. This absorption front is an important mechanism of energy deposition during a laser damage initiation event on the exit surface of SiO_2 for ns pulses. The absorption front moves nearly linearly in time and is strongly intensity dependent, and is hence laser driven. The physics which drives the absorption front is temperature activated absorption and temperature activated free electron conductivity. This model provides a framework for full laser damage models be capturing the primary mechanisms of energy deposition and transport during damage.

V. REFERNCES

[1] C. W. Carr and J. M. Auerbach., Optics Letters 31, 595 (2006).

[2] R. A. Negres, M. D. Feit, P. DeMange, J. D. Bude, and S. G. Demos, "Pump and probe damage testing for investigation of transient material modifications associated with laser damage in optical materials", SPIE, 72019, (2008)

[3] C. W. Carr, M.J. Matthews, J.D. Bude, and M.L. Spaeth, "The effect of laser pulse duration on laser-induced damage in KDP and SiO_2",SPIE 6403, K4030 (2007).

[4] C. W. Carr, H. B. Radousky, and S. G. Demos, Phys Rev Lett **91** (12), 127402 (2003)

[5] M. D. Feit and A.M. Rubenchick, “Implications of nanoabsorber initiators for damage probability curves, pulselength scaling and laser conditioning” SPIE 5273, 74, (2004);

[6] M. C. Nostrand, T. L. Weiland, R. L. Luthi, J. L. Vickers, W. D. Sell, J. A. Stanley, J. Honig, J. Auerbach, R. P. Hackel, and P. J. Wegner, “A large aperture, high energy laser system for optics and optical component testing”, SPIE 5273, 325 (2003).

[7] J. Bude, G. Guss, M. Matthews, and M. L. Spaeth, “The effect of lattice temperature on surface damage in fused silica optics”, SPIE 6720, 72009. (2008)

[8] C.W. Carr, J.Bude, P. Demange, “Laser-supported solid-state absorption fronts in silica”, In Press Physical Review B

[9] C. W. Carr, H. B. Radousky, A. M. Rubenchik, M. D. Feit, and S. G. Demos, Phys Rev Lett 92 (8), 087401 (2004).

[10] S. T. Yang, M.J. Matthews, S. Elhadj, V.G. Dragoo, S.E. Bisson, J. of Applied Physics 106, 103106 (2009).

[11] D. G. Hicks, T.R. Boehly, J.H. Eggert, J.E. Miller, P.M. Celliers, and G.W. Collines, Physical Review Letters 97, 025502 (2006).

[12] C. W. Carr, M.D. Feit, M.A. Johnson, and A.M. Rubenchik, Applied Physics Letters 89, 131901 (2006).

[13] K. Saito and A.J. Ikushima, Physical Review B 62, 8584 (2000).

[14] D. Arnold and E. Cartier, Physical Review B 46, 15102 (1992).

[15] K. Hess, Theory of Semiconductor Devices (IEEE Press Marketing, Piscataway, NJ, 2000).

[16] C. W. Carr, H.B. Radousky, A.M. Rubenchik, M.D. Feit, S.G. Demos, Physical Review Letters 92, 087401 (2004).

[17] D. A. Young and E. M. Corey, “A new global equation of state model for hot, dense matter,” Journal of Applied Physics, Vol. 78, No. 6, 15 Sept. 1995.]